Labeling of Cells with Silver and Gold Host-Guest Nanocomposites

Lajos P. Balogh [*], Wojciech Lesniak [*], Vladimir A. Sinani[*], Anna U. Bielinska**, Kai Sun***, Bindu M. Nair[*], Emily Waite[*], Muhammed S. T. Kariapper[*], and Mohamed K. Khan[*]

[*] The NanoBiotechnology Center at Roswell Park Cancer Institute (NBC at RPCI), Department of Radiation Medicine, Roswell Park Cancer Institute, Buffalo, NY, USA, Lajos.Balogh@roswellpark.org
[**] Michigan Nanotechnology Institute for Medicine and Biological Sciences, University of Michigan, Ann Arbor, MI, USA
[**] Electron Microbeam Analysis Laboratory, University of Michigan, Ann Arbor, MI, USA

ABSTRACT

Nanocomposites combine the properties of nano-sized inorganic guest atoms/molecules with their nanoscopic size polymer host. Using poly(amidoamine) (PAMAM) dendrimers as templates we have synthesized water-soluble, biocompatible, fluorescent, and stable nanocomposites with regulated surface charge and controlled size for cell labeling studies. Silver {Ag^0-PAMAM} and gold {Au^0-PAMAM} dendrimer nanocomposites were used for in vitro cell labeling. The results indicate that surface charge plays a significant role in biocompatibility and cellular internalization. Cytotoxicity (or lack thereof) of the host dendrimers and related nanocomposites was evaluated in normal and cancer cells using XTT assay. Cellular uptake of nanoparticles was examined by TEM and confocal microscopy. We demonstrate that nanocomposites can be used as cell biomarkers.

Keywords: poly(amidoamine) dendrimer, silver and gold/dendrimer nanocomposite, cell labeling

1 INTRODUCION

Quantitative imaging of cancer is a highly desired tool for diagnosis. Traditionally various fluorescent dyes are used to label nanodevices providing spectacular intracellular images and revealing cellular details. However, quantification of amounts internalized by cells is often problematic because of photobleaching. Quantum dots (semiconductor crystalline nanoparticles) that have been used recently do not photobleach, but may potentially be sensitive to decomposition[1]. Small noble metal nanoparticles of Ag and Au have been reported to be fluorescent and they have high quantum yields[2].

It has been shown that poly(amidoamine) (PAMAM) dendrimers are ideal templates for metal nanoparticles due to their highly regular, branched, three-dimensional structure. The resulting organic/inorganic composite nanoparticles contain guest atoms as amorphous or irregular nanoclusters topologically trapped in dendritic polymer hosts of well-defined size, charge, and terminal functionality [3-6]. The host can be made in discrete sizes, regulated surface charges, and functionalities. The design of these nanodevices permits the host and guest properties to be individually modified and optimized.

2 EXPERIMENTAL

Using PAMAM dendrimers with different terminal groups, we have synthesized water-soluble, fluorescent, and stable nanocomposites with regulated surface charge (positive, neutral and negative) in controlled sizes for cell labeling studies. Silver and gold nanocomposites were prepared as described in our previouos reports7,8. They were characterized by means of UV-vis spectroscopy, fluorescence spectroscopy, dynamic light scattering, zeta potential measurements, high-resolution transmission electron microscopy, X-ray energy dispersive spectroscopy, and selected area electron diffraction. The cytotoxicity of dendrimers and related silver nanocomposites was evaluated using a colorimetric assay of cellular viability. For in vitro labeling, the cell cultures (Rat2, MatLyLu prostate cancer cells, B16 melanoma cells, and human dermal microvascular endothelial cells) were incubated with varying concentrations of dendrimers ("host only") or nanocomposites. XTT cell viability assay was used to measure the number of intact cells for both hosts and host-guest structures. Cellular internalization of {Ag(0)} and {Au(0)} nanocomposites was observed by TEM[7,8].

3 RESULTS AND DISCUSSION

We have found that the size distribution of nanoparticles, as well as their surface charge, is determined by the type and number of terminal groups of the dendrimer templates (Table1). {$(Au^0)_{10}$-PAMAM_E5.NH_2}, and {$(Au^0)_{25}$-PAMAM_E5.NH_2} nanocomposites are positively charged at pH 7.4, (including{$(Au^0)_{25}$-PAMAM_E5.NGly}, which is slightly positive), because primary and secondary amino groups of the dendrimer hosts are partially protonated at this biologic pH value. The systems display narrow size distribution, with single particles of low scattering efficiency and a small fraction of higher order aggregates that exhibit strong light scattering. As expected, {$(Au^0)_{25}$-PAMAM_E5.SAH} nanocomposite particles carry a net negative charge because the vast majority of carboxyl groups of dendrimer template is deprotonated at pH=7.4. These composite nanoparticles display stronger tendency to form higher order aggregates (as also observed in TEM, data not shown).

$\{(Ag^o)_{25}PAMAM\_E5.NH_2\}$ nanocomposite exhibited

Nanocomposite	Number Weighted Average (nm)	Volume Weighted Average (nm)	Intensity Weighted Average(nm)	Zeta Potential (mV)
$\{(Au^0)_{10}E5.NH_2\}$	13.4 (100%)±1.4	14.0 (99.4%)±1.9	11.8 (4.9%)±1.3 111.8 (95.1%)±15.2	+23.3
$\{(Au^0)_{25}E5.NH_2\}$	10.8 (99.6%)±0.8 37.8 (0.4%) ±2.3	11.1 (83.7 %)±1 38.71 (15.5%)±3.3 149 (0.8%)±18.6	11.3 (4%) ±1 40.5 (29.9%) ±3.8 154.6 (66.1%)±17.5	+19.45
$\{(Au^0)_{25}E5.NGly\}$	11.5 (100%) ±1.6	12.2 (94.8%)±1.5 107.5 (5.2%)±12.2	12.8 (2.9%)±1.3 111.8 (97.1%)±15.2	+5.93
$\{(Au^0)_{25}E5.NSAH\}$	10.9 (96) ±0.8 27.1 (4%) ±3	11.1 (55.3%)±1.9 28.5 (42.3%)±4.3 134.8 (3.7%)±14.2	11.4 (1.14%)±0.9 29.7 (11.9%)±3.5 139.7 (87%)±17.5	-18.17

Table 1: Summary of dynamic light scattering and average zeta potential data of nanocomposites obtained for 1 mg/mL aqueous solution.

Silver/dendrimer nanocomposites have been reported to be fluorescent9,10. The $\{(Ag^0)_{25}$-PAMAM_E5.$NH_2\}$, $\{(Au^0)_{25}$-PAMAM_E5.NGly}, and $\{(Au^0)_{25}$-PAMAM_E5.NSAH} nanoparticles could be excited in wavelengths ranging from 300 nm to 400 nm, resulting in emissions in the range of 400 - 500 nm, confirming previous reports. Prompted by the fluorescence properties of silver nanocomposites, we further studied these materials in terms of their potential application in biologic systems as biomarkers that can be observed both by fluorescence spectroscopy and TEM. As the first step, the cytotoxicity of the PAMAM_E5.NH_2, PAMAM_E5.NGly, and PAMAM_E5.NSAH dendrimer templates and their silver or gold composites were examined in KB cell culture using XTT colorimetric assay of cellular viability7,8. Cytotoxicity of nanocomposites was found to essentially be the same as of the host. DNCs as cell labels were further studied by confocal microscopy. Rat2 cell culture was incubated with either dendrimers or their corresponding silver DNCs for 2 h at 37 C in PBS buffer (pH 7.4) at 100 nM, 500 nM and 1000 nM concentrations. To test the possibility of using confocal microscopy to visualize silver/dendrimer nanocomposites, a drop of aqueous solution of each DNC was placed on microscopy cover glass and mixed with a prolonged kit. After condensation, the samples were analyzed using Zeiss LSM 510 confocal microscope. (Fig. 1A, inverted image).

In the nanocomposite containing samples, regions exhibiting relatively strong fluorescence could be detected, but not in samples of dendrimer templates. Similar results were obtained for PAMAM_E5.SAH, $\{(Ag^0)_{25}$-PAMAM_E5.NSAH}, and PAMAM_E5.NGly, $\{(Ag^0)_{25}$-PAMAM_E5.NGly} materials. Figure 1 B and C display inverted fluorescence (left panels) and DIC (right panels) images of Rat2 cells incubated with 500 nM of $\{(Ag^0)_{25}$-PAMAM_E5.$NH_2\}$ nanocomposite, and a control sample, respectively. Both sets were collected under the same experimental conditions. Cells incubated with measurable intracellular fluorescence proving that (a) the fluorescence is not quenched and (b) the nanoparticles were internalized within the cells and are visibly located in the cytoplasm.

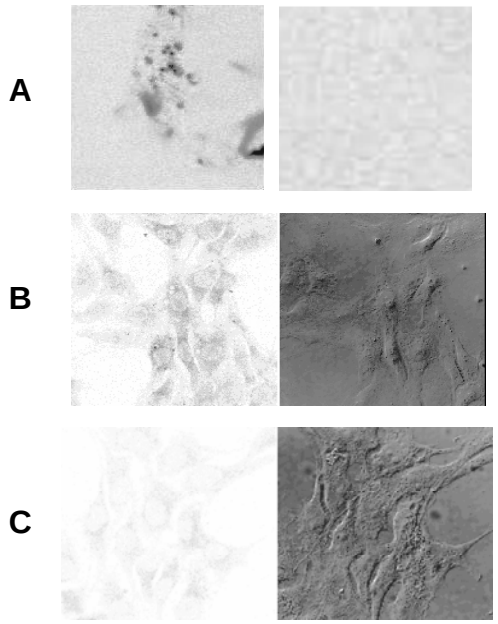

Figure 1: Inverted confocal microscopy images. A. PAMAM_E5.NH_2 (right panel - no fluorescence was detected) and $\{(Ag^0)_{25}$-PAMAM_E5.$NH_2\}$ (left panel, areas exhibiting intense fluorescence can be clearly seen) mixed with prolong anti fade kit; B. Rat2 cells incubated with $\{(Ag^0)_{25}$-PAMAM_E5.$NH_2\}$ nanocomposite at concentration of 500 nM for 2 h at 37 C in PBS, pH 7.4, recorded in the fluorescence (left panel) and DIC (right panel) modes; C. Control cells. Significant increase of intracellular fluorescence in cells incubated with $\{(Ag^0)_{25}$-PAMAM_E5.$NH_2\}$ nanocomposite compared to control cells was observed[7].

There are also small areas exhibiting relatively strong fluorescence; we speculate that these areas might

correspond to the nanocomposite aggregates trapped in the endocytic or phagocytic vesicles, as seen also in TEM images. Similar results were obtained for the negatively charged $\{(Ag^0)_{25}$-PAMAM_E5.NSAH$\}$ DNC, while - interestingly - incubation of Rat2 cells with the nearly neutral $\{(Ag^0)_{25}$-PAMAM_E5.NGly$\}$ nanoparticles did not result in elevated intracellular fluorescence, possibly due to low uptake.

A few atoms of sliver or gold per PAMAM dendrimer already make possible the visualization of the amorphous single and multiple nanocomposite units both in tissues and in cells by electron microscopy. A typical high resolution TEM image of a positively charged $\{(Au^0)_{10}$-PAMAM_E5.$NH_2\}$ is shown in Figure 2.

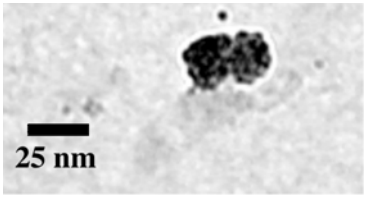

Figure 2: Comparison of a single $\{(Au^0)_n$-E5.$NH_2\}$ particle and a $(\{Au\}_n)_2$ a dimer of nanocomposite clusters[8].

The size distribution tends to be uniform, although an extensive amount of aggregation may occur on the carbon coated TEM grid similar to those observed in the literature[11]. Similar results were obtained for silver nanocomposites. This characteristic size, shape and contrast make the observation of silver and gold nanocomposites simple by electron microscopy. Furthermore, no other objects can be found in tissues or cells that are similar in shape, size and especially contrast to the {Ag} or {Au} nanocomposites. DNCs can have a specific charge on their host polymer and therefore may be used to map certain cell compartments and cellular structures. These local interactions may be induced by either charge or surface (p_H or protein content). Interacting cellular structures that are preferred by various nano-particles can be made visible this way. These local interactions may be induced by either charge or surface (p_H or protein content).

Figure 3 displays representative TEM images collected for NIH3T3 (A, B) and U937 (C, D) cell lines incubated with $\{(Ag^0)_{25}$-PAMAM_E5.$NH_2\}$ nanoparticles. After 1 h incubation at 37^o C, {Ag} nanocomposite particles were observed in the form of randomly dispersed single particles or agglomerates on the surface of cellular membranes, in the cytoplasm, or trapped by the phagocytic or endocytic vesicles. It seems that internalization of the polycationic $\{(Ag^0)_{25}$-PAMAM_E5.$NH_2\}$ nanoparticles may occur through two distinct mechanisms: both phagocytosis and diffusion via cell walls. Similar results were obtained for the polyanionic $\{(Ag^0)_{25}$-PAMAM_E5.NSAH$\}$ nanocomposite, whereas cellular uptake of the neutral $\{(Ag^0)_{25}$-PAMAM_E5.NGly$\}$ was low.

Further we have used reporter plasmid DNA and positively charged gold $\{(Au^0)$-PAMAM_E5.$NH_2\}$ nanocomposites to visualize the intracellular trafficking of DNA/PAMAM dendrimer complexes.

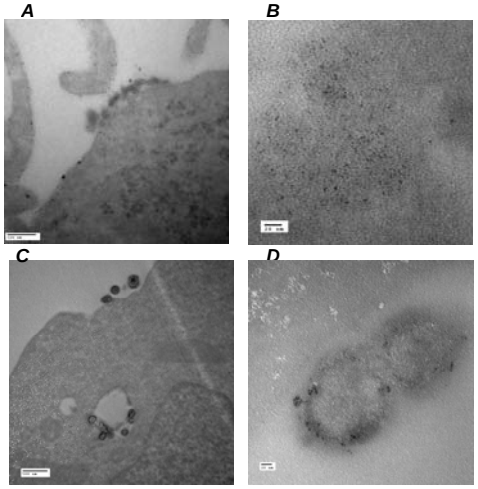

Figure 3: Representative TEM images of NIH3T3 and U937 cell lines incubated with $\{(Ag^0)_{25}$-PAMAM_E5.$NH_2\}$ nanoparticles for 1 h at 37 C and at 500 nM DNC concentration. A and B - NIH3T3 cell showing DNCs located on the surface of the cell and randomly dispersed single particles in the cytoplasm respectively; C and D U937 cell viewing the agglomerates of DNCs located on the surface of the cell and trapped in the phagocytic or endocytic vesicles[7].

Complexes of plasmid DNA (pCF1/LUC; 5.5 kb) and gold nanocomposite of $\{(Au^0)_{10}$–PAMAM_E5.$NH_2\}$ were formed in double distilled H_2O at a 10:1 ({Au}:pDNA) charge ratios, which represent the typical condition of complex formation. Gene transfections were performed by incubating the complexes with Cos-1 cells (monkey kidney fibroblasts; 1 x 105 cells/cm3) for three hours at 37˚C. Cells were washed and grown overnight (24 hrs, 37˚C) in growth medium supplemented with 10% FBS. The luciferase expression was found comparable to that in the control transfections performed by using regular PAMAM_E5.NH_2 (Figure 4).

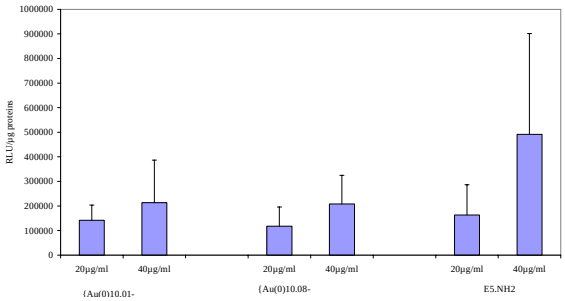

Figure 4: In vitro transfection using PAMAM dendrimers and their gold nanocomposites[8].

This indicated that presence of metal component in the {Au} nanocomposite does not inhibit processes of transfer, subsequent transcription and translation of the introduced

DNA. We have not observed any increase in toxicity due to the metal content of gold nanocomposites indicating that toxicity of these nanomaterials is determined by the dendrimer used. The luciferase expression was found comparable to that in the control transfections performed by using regular PAMAM_E5.NH_2.

This indicated that presence of metal component in the {Au} nanocomposite does not inhibit processes of transfer, subsequent transcription and translation of the introduced DNA. We have not observed any increase in toxicity due to the metal content of gold nanocomposites indicating that toxicity of these nanomaterials is determined by the dendrimer used.

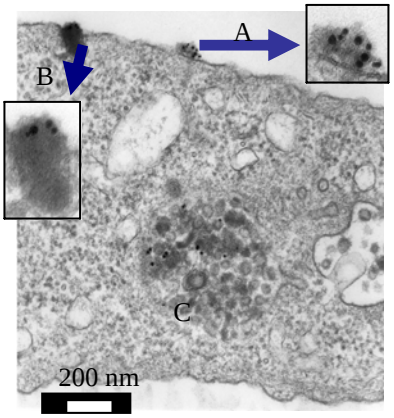

Figure 5: Visualization of gene transfection with plasmid DNA-gold/PAMAM nanocomposite complexes. A: Cell surface attachment, B: Complex just undergoing endocytosis, C: Complexes localized in lysozome[8].

Figure 5 illustrates all these three steps. Interestingly, the original distribution of the highly visible $\{Au\}_n$ clusters is clearly random in the pDNA-{Au} complexes. However, images taken at a later time indicate the movement of the dark nanoparticles toward the internal surface of the lysozomal vesicles indicating flow characteristic of a living cell (Figure 6).

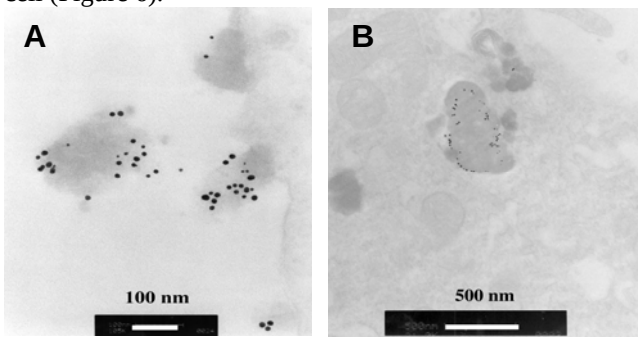

Figure 6: A. Random distribution of {Au}n nanocomposite clusters before and during cell surface attachment. B. Arranged near the internal membrane of the lysozome after approximately four hours.

To examine {Au} localization by transmission electron microscopy, Jurkat cells were fixed at 4˚C in 2.5% glutaraldehyde and post-fixed in 1% osmium tetroxide. Selected samples were *en bloc* stained with 3% uranyl acetate. Ultra-thin sections were examined on a Philips CM100 TEM. $\{Au\}_n$ clusters appear as 25-30 nm dark spots while $\{Au\}^+$ positively charged single gold/dendrimer nanocomposites interacting with several pDNA molecules that result in the gray stain of the complex. Only multiple pDNA/$\{Au\}^+$ complexes were observed under the experimental conditions we used. Initially these complexes were found attached to the cell surface. Then, they were subsequently endocytosed and they entered lysosomal compartment of cells.

4 SUMMARY

Presented results indicate that toxicity and cellular uptake of investigated silver and gold DNCs correlate with the surface charge of nanoparticles. Moreover, positively charged gold/PAMAM nanocomposites used as DNA carriers were capable of gene transfection with efficiencies similar to their host dendrimer. It appears that in contrast to general beliefs, nanocomposites as well as large pDNA-PAMAM clusters (containing many DNA molecules and many dendrimers) undergo endocytosis after surface binding. The diffusion of various dendrimer nanocomposites is controlled by the polymer host and not by the inorganic guests. By varying the charge and lipophilicity of the host, the particle can enter into interaction with various biologic entities.

REFERENCES

[1] M. Stroh, J. P. Zimmer, D. G. Duda, T.S. Levchenko, K. S. Cohen, E. B. Brown, D. T. Scadden, V. P. Torchilin, M. G. Bawendi, D. Fukumura, R. K. Jain, Nat. Med. May 1-5, 2005.

[2] Z. Zheng, J. Petty and R.M. Dickson, J. Am. Chem. Soc. 125, 7780, 2003.

[3] L. P. Balogh, S. S. Nigavekar, A. C. Cook, I. Minc and M. K Khan. Proceedings of ACS PMSE 77, 118, 1997.

[4] M. Zhao, L. Sun and R. M. Crooks, J. Am. Chem. Soc. 120, 4877, 1998.

[5] L. Balogh, D.A. Tomalia, IBID 120, 7355, 1998.

[6] K. Esumi, A. Suzuki, N. Aihara, K. Usui, K. Torigoe, Langmuir 14, 3157, 1998.

[7] W. Lesniak, X. Shi, A. U. Bielinska, K. W. Janczak, K. Sun, Jr. J. R. Baker and L. P. Balogh, Nano Letters 5, 2123, 2005.

[8] A. Bielinska, J. D. Eichman, I. Lee, J. R. Baker, Jr. and Lajos Balogh , J. of Nanoparticle Res., 4, 395, 2002.

[9] A. Mostafa, M. El-Sayed, A. Acc. Chem. Res. 37, 326 2004.

[10] P. Fevre, L. H. Magnan, A. Midoir, D. Chandesris, H. Jaffres, A. R. Fert, J. P. Peyrade, Surf. Rev. Let., 6, 753,1999.

[11] F. Gröhn, B. J. Bauer, Y. A. Akpalu, C. L. Jackson, E. J. Amis, Macromolecules 33, 6042, 2000.